HHS Public Access

Author manuscript

J Occup Environ Hyg. Author manuscript; available in PMC 2019 March 01.

Published in final edited form as:

J Occup Environ Hyg. 2018 March ; 15(3): 214–225. doi:10.1080/15459624.2017.1411597.

Comparison of the CAS-POL and IOM samplers for determining the knockdown efficiencies of water sprays on float coal dust

Clara E. Seaman, **Michael R. Shahan**, **Timothy W. Beck**, and **Steven E. Mischler**

Pittsburgh Mining Research Division, NIOSH, Pittsburgh, Pennsylvania

Abstract

Float coal dust, generated by mining operations, is distributed throughout mine airways by ventilating air designed to purge gases and respirable dust. Float coal dust poses an explosion hazard in the event of a methane ignition. Current regulation requires the application of inert rock dust in areas subjected to float coal dust in order to mitigate the hazard. An alternate method using water sprays, which have been effective in controlling respirable dust hazards, has been proposed as a way to control float coal dust generated on longwall faces. However, the knockdown efficiency of the proposed water sprays on float coal dust needs to be verified. This study used gravimetric isokinetic Institute of Occupational Medicine (IOM) samplers alongside a real-time aerosol monitor (Cloud Aerosol Spectrometer with polarization; CAS-POL) to study the effects of spray type, operating pressure, and spray orientation on knockdown efficiencies for seven different water sprays. Because the CAS-POL has not been used to study mining dust, the CAS-POL measurements were validated with respect to the IOM samplers. This study found that the CAS-POL was able to resolve the same trends measured by the IOM samplers, while providing additional knockdown information for specific particle size ranges and locations in the test area. In addition, the CAS-POL data was not prone to the same process errors, which may occur due to the handling of the IOM filter media, and was able to provide a faster analysis of the data after testing. This study also determined that pressure was the leading design criteria influencing spray knockdown efficiency, with spray type also having some effect and orientation having little to no effect. The results of this study will be used to design future full-scale float coal dust capture tests involving multiple sprays, which will be evaluated using the CAS-POL.

Keywords

Coal mining; dust explosion; dust suppression; gravimetric sampling; real-time aerosol monitor

CONTACT Clara E. Seaman, CESeaman@cdc.gov, Pittsburgh Mining Research Division, NIOSH, 626 Cochrans Mill Rd., Pittsburgh, PA 15236.

Disclaimer

The findings and conclusions in this article are those of the authors and do not necessarily represent the views of the National Institute for Occupational Safety and Health. Mention of company names or products does not constitute endorsement by the National Institute for Occupational Safety and Health.

Color versions of one or more of the figures in the article can be found online at www.tandfonline.com/uoeh.

ORCID

Clara E. Seaman http://orcid.org/0000-0002-0166-3549

Introduction

Mining operations generate float coal dust (FCD), diameter <75 μm, which is transported by ventilating air designed to purge methane and other respirable aerosols from the mine airways. This float coal dust eventually settles on the floor, ribs, and roof of mine entries. In the event of a methane explosion, this dust may become re-entrained and, if sufficient concentrations exist, fuel a secondary dust explosion that may propagate throughout the mine.[1,2] FCD-related explosions were responsible for 18% of U.S. coal mining-related fatalities between 2001 and 2010.[3,4] In order to protect against potentially explosive concentrations of FCD, U.S. mine operators are required to maintain at least 80% incombustible material on all mine surfaces, which is achieved through the application of inert rock dust (e.g., limestone).[5] However, in the case of longwall mines it may be possible to reduce the amount of FCD that settles in the mine airways by developing strategies to limit the amount of dust that leaves the active mining face and enters the return.

Water sprays have proven to be an effective method for controlling thoracic (50% cut point 10 μm) and respirable (50% cut point = 4 μm) dust=either by redirecting the dust or by actively knocking the dust from the air.[6] Scavenging of coal dust by water droplets arises through one of three modes of deposition: diffusion, interception, and inertial impaction.[7,8] Inertial impaction and diffusion both rely on the deviation of the coal dust from its streamline. For sub-micron particles, this occurs by diffusion.[9,10] Larger heavier particles have enough inertia to prevent them from following the curve of the streamline around individual water drops, resulting in collisions where the resulting agglomerate settles quickly out of the airstream.[10–12] Interception occurs when a particle that remains on its streamline strikes the droplet.[10,13] The collective measure of these three modes of deposition by a water spray is the collection or knockdown efficiency (KE) of the spray. Using respirable coal dust, it has been found that the KE of a spray is directly proportional to operating pressure, water flow rate, and droplet velocity, and inversely proportional to air flow rate and mean droplet diameter.[14–17] Increasing water pressure leads to increased droplet velocity and decreased droplet diameter, both of which improve KE. This trend does not increase indefinitely; it was found that, for an open air spray system operating at 2757 kPa (400 psi), the airflow generated by the sprays diluted the dust concentrations to the point where KE became greatly reduced.[18] Similarly, while smaller droplets tend to lead to increased KE, decreasing droplet size also leads to a decrease in droplet momentum, thus reducing the collision velocity and droplet penetration into the dust cloud, which can reduce the KE.[16,19] Examination of nozzle type found that air atomizing and hollow cone sprays removed more respirable dust than flat fan or full cone sprays on a per-unit-volume-of-water basis.[20,21] A more recent NIOSH study examined seven sprays commonly found in the mining industry by analyzing spray droplet size and mean droplet velocity in order to better understand dust capture effectiveness.[22] This study found that an increase in pressure led to an increase in droplet velocity and a decrease in droplet size. Additionally, this study found that droplet size was inversely related to induced airflow while droplet velocity was directly related to dust removal.

While detailed analyses have been conducted on the findings of these studies with respect to respirable dust, these findings need to be verified with respect to airborne FCD, as FCD

contains larger particles that may interact with the water sprays differently. Additionally, there is a relationship between the lean flammable limit and the size of dust particles, with smaller dust having increased flammability, indicating a need to further understand how the water sprays affect dust over different size ranges.[23–25] Previous studies that focused on characterizing respirable dust exposures used gravimetric techniques with respirable samplers to provide time-averaged mass concentration measurements as the primary method for determining spray efficiency. While gravimetric samplers capable of measuring total dust exist, they are unable to resolve the knockdown efficiencies on total airborne coal dust based on the size distribution and location of dust particles across the longwall entry cross section. To achieve simultaneous size distribution and location data, a real-time aerosol monitor must be used. Another benefit of real-time monitors is that test results can be evaluated immediately following the test completion, unlike gravimetric filters which may require multiple days for processing. Optical spectrometers can provide real-time measurements for a wide size range of aerosols, but require extensive calibration to ensure accurate particle sizing.[26–28]

NIOSH acquired a Cloud, Aerosol, and Precipitation Spectrometer (CAPS; Droplet Measurement Technologies Boulder, CO), which is designed for *in situ* atmospheric aerosol sampling and is capable of measuring real-time size distributions of atmospheric aerosols through forward light scattering.[29] The CAPS consists of two different instruments: the Cloud Imaging Probe (CIP) and Cloud Aerosol Spectrometer with Polarization (CAS-POL). The CIP measures particles in the 12.5–1.55 mm range, while the CAS-POL is able to measure particles size between 0.51 μm and 50 μm. The CIP was not used for this study because it is unable to resolve the morphology of sub-75 μm particles, while a depolarization module in the CAS-POL allows for classification of particle morphologies and composition.[30–33] NIOSH calibration experiments of the CAS-POL using size-selected coal dust demonstrated that the CAS-POL was capable of sizing coal dust particles by analyzing forward light-scattering measurements with T-matrix (sub-1.5 μm) and ray tracing with diffraction on facets (RTDF) (1.5–75 μm) theories for irregular particles.[34] While the coal dust calibration tests focused only on the use of forward scattered light to estimate particle size, the current study also analyzes the backscattered and polarized light to classify particles according to shape and composition, as both coal dust and water droplets are present during each knockdown test. Therefore, it is necessary to distinguish between coal and water in order to accomplish the following two goals.

1. To determine the efficacy of using the CAS-POL as compared to the IOM samplers for investigating the KE of mining dust controls.
2. To examine the knockdown efficiency (KE) of seven different mining water sprays under different operating conditions.

The spray KE as measured by the CAS-POL will be statistically compared to the KE measured by IOM gravimetric samplers to determine the degree of agreement between the two methods, while the information obtained on the spray KE will be used to design a full-scale water curtain for use in underground coal mines.

Methods

Experimental setup

All tests were conducted at a full-scale longwall gallery test facility at the National Institute for Occupational Safety and Health (NIOSH) Pittsburgh Mining Research Division. The simulated face is 38.1 m long by 5.5 m wide and 2.29 m high from floor to roof. Nineteen mock 1.8-m longwall shields cover the length of the longwall section, and a full-scale mock-up Joy 7LS double ranging arm shearer is located approximately halfway between the headgate and tailgate of the testing gallery. Brattice curtain was suspended from the shields, spanning from shield 11 to shield 3, creating a tunnel 1.7 m high by 0.91 m wide that minimized irregularities in the airflow due to the shearer (Figure 1). Ventilation of the tunnel was set to 3.5 m/s.

FCD was introduced to the test section at the center of shield 9 near the entrance of the brattice tunnel. The release point was directed such that dust was ejected along the tunnel centerline 0.51 m from the underside of the shield canopy. Dust was generated by using a screw-type feeder system with coal dust funneled into an eductor that used compressed air to carry the dust through hoses to the release point in the gallery. The coal dust supplied to the feeder (mean: 23.02 μm, SD: 18.22 μm) was custom-milled to contain float-dust-sized particles. The screw feeder feed rate was adjusted so as to achieve an average respirable dust concentration of 6.0 mg/m^3 as measured using a pDR-1000 real-time monitor (ThermoFisher Scientific, Waltham, MA) at the gallery tailgate. This dust concentration was similar to the levels observed during a longwall survey conducted by NIOSH researchers.[35]

Seven water sprays were selected for this study (Table 1). The sprays were attached in pairs to an adjustable angle mounting plate (ThorLabs Inc., Newton, NJ) that allowed the sprays to be positioned at 45° with or against the airflow. The mounting plates were magnetically attached along the tunnel centerline to the underside of shield 8, 1.5 m from the dust source. A second pDR-1000 was placed between the dust source and spray. The water pressure was set to either 552 kPa for single fluid sprays and 172 kPa for both water and air for the twin fluid spray during the low-pressure tests and 1104 kPa for single-fluid sprays and 345 kPa for the twin-fluid spray during the high-pressure tests.

Located between shields 2 and 3 was a planar motion system, as noted in Figure 1. The system consists of a 5-m horizontal track and a cart built out of 80–20 aluminum extrusion. The cart holds a custom-built vertical sled system with a 1.6-m range of motion. Both the cart and sled were driven by NEMA 34 high-torque stepper motors (Applied Motion, Watsonville, CA) capable of achieving a 20,000 micro-step resolution and controlled using STAC6 stepper drives (Applied Motion, Watsonville, CA) using serial commands. A custom LabVIEW virtual instrument was created to automate the motion of the cart and sled, allowing for precise and repeatable positioning of the sled, which carried the instrumentation used to evaluate the knockdown efficiencies of the spray.

The primary instrument used for measuring KE was the CAS-POL, which uses forward light scattering to measure particle sizes and polarized backscattered light to classify according to morphology and composition.[32] The CAS-POL uses sensors to collect forward (4–12°) and

backscattered (168–176°) light from each particle that passes through a laser beam with a wavelength of 658 nm. The forward detector is used to size the particles, while the backscattered light is split into parallel (P) and perpendicular (S) components for morphology estimations as described in the Data Analysis section below.

The secondary method of evaluating the spray efficiencies used total dust samplers to collect airborne dust during each phase of testing.[36] Three IOM samplers, each containing a 25-mm quartz fiber filter and fitted with an isokinetic nozzle, were positioned 6.4 cm apart on a mounting bracket 10 cm above the CAS-POL portion of the CAPS instrument (Figure 1). Each sampler was connected to a critical flow orifice, regulating the flow through the sampler to 2 L/min. The filters were desiccated overnight and then conditioned for 24 hr in a temperature- and humidity-controlled clean room before weighing.

A full factorial design was used to test the effects of spray type, orientation, and pressure on the KE of each spray. Tests were replicated three times and order was randomized. Each test consisted of three phases: dust-only, spray-only, and knockdown (dust and spray). The tunnel was segmented based on EPA Method 1 into 15 equally sized windows.[37] Measurements were collected for one minute at the center point of each location for each test phase.

Data analysis

To determine the KE of each spray, coal particles needed to be distinguished from water particles during the knockdown phase of each test and then compared to the number of particles that occurred during the dust-only phase of the same test. Previous studies have compared the polarization ratio of different particles to determine particle type.[31,38–41] The polarization ratio, δ, is defined as

$$\delta = \frac{S}{S+P}, \quad (1)$$

where P is the parallel polarized light and S is the perpendicularly polarized light. The CAS-POL laser used in this study was linearly polarized; it is expected that an aspherical particle, such as coal dust, will scatter the S and P components unequally, distinguishing it from a water droplet.[42] The wide range of particle sizes and shapes measured in this study resulted in a larger degree of overlap between the optical signature of the coal dust and water than was expected. The dust-only and water-only phases were used to determine the size and polarization ratio values where only coal dust occurred. This was done by subdividing the data from the dust-only and water-only phases by the forward scattering count value and the polarization ratio. The step resolution used to subdivide the data was 10,000 counts for the forward scattering data and 0.1 for the polarization ratio. Regimes that consisted primarily of coal dust (at least 90%) were saved and applied to the data obtained during the knockdown phase. Any particle that resided in these locations during the knockdown phase was classified as coal. Once particle type and size were determined, spray KE by count was calculated as

$$KE_{CAS-POL,count} = \frac{N_{Coal} - N_{Knockdown}}{N_{Coal}} * 100, \quad (2)$$

where $N_{Knockdown}$ is the number of coal dust particles counted during the knockdown tests, and N_{Coal} is the number of coal dust particles counted during the dust-only test that do not occur in regions indistinguishable from water. An examination into the effects of misclassifying water by this method was conducted. KE by count was calculated during the knockdown phase first by assuming that all water particles dropped out before reaching the CAS-POL, and second by assuming that no particles of water dropped out before reaching the CAS-POL. The former case would provide a maximum underestimation, because some water would be misclassified as coal, thus reducing the apparent KE, while the latter case would provide a maximum overestimation as some coal particles would be misclassified as water. The $KE_{CAS\text{-}POL,count}$ was then compared to these values and it was found that the calculated CAS-POL KE tended toward underestimation in 66% of the cases and towards overestimation in 33% of the cases.

Volume equivalent diameters of the water particles were estimated by Mie calculations using the scattering cross section measured by the CAS-POL.[43] For dust particles with scattering cross sections 1.5 μm, T-matrix theory was used to calculate the volume equivalent diameter of the coal particle, while dust particles larger than 1.5 μm were sized using the RTDF method. RTDF and T-matrix theories were selected for use with coal dust because they have been successfully used to estimate volume equivalent diameters from optical scattering cross sections for other types of faceted, irregularly shaped particles such as volcanic ash and mineral dust aerosols.[39,44,45] Using the volume equivalent diameters, the mass of each coal particle was estimated (ρ = 1.3738 g/cm^3) and used to calculate an KE by mass ($KE_{CAS\text{-}POL,mass}$) for comparison to traditional gravimetric sampling methods such as the IOM sampler.[46] KE as determined by the IOM sampler was defined as

$$KE_{IOM} = \frac{M_{Coal} - (M_{Knockdown} - M_{Water})}{M_{Coal}} * 100, \quad (3)$$

where $M_{Knockdown}$ is the mass of material collected on the filter during the knockdown phase, M_{water} is the mass of material collected on the filter during the water-only phase, and M_{Coal} is the mass of material collected on the filter during the coal-only phase.

During preliminary testing, it was found that the water used during testing left a measurable residue on the filters, which in some cases was significant enough to be confounded with the change in dust mass due to the control. Therefore, filters were also used during the water-only phase to establish a correction factor for each spray. This correction factor was subtracted from overall mass measured on the filter during the knockdown phase to find the portion of the mass gain that was attributed only to coal dust. Due to the additional sizing information from the CAS-POL, KE values based on mass and count were calculated for three different ranges of particle sizes. Statistical analysis of the results was performed using

SAS 9.4 (SAS Institute Inc., Cary, NC) and a p-value of 0.05 was used as the threshold of significance.

Particle sizes bin selection

The numbers of particles counted for each test phase for all the tests conducted are shown in Figure 2. The particles were separated into three different size bins for this study. The first bin was set to include particles ≤4 μm. This threshold was chosen as it represents the 50% cut size of the international definition for respirable aerosol sampling.[47,48] The second bin size consisted of particles >4 μm and ≤20 μm. The threshold of 20 μm represents the 98th percentile of lognormal distribution that fits the frequency histogram for particles greater than 4 μm, and matches the 50% cut point of an airborne dust sampling cyclone used during NIOSH FCD field surveys.[35] The final bin contains the remaining and largest particles that were measured during testing.

Results and discussion

Overall KE

CAS-POL vs. IOM samplers—Regression analysis on both the $KE_{CAS\text{-}POL,mass}$ and KE_{IOM} data found that spray type ($p_{CAS\text{-}POL,mass}$ 0.0001, $p_{IOM} < 0.0001$) and pressure ($p_{CAS\text{-}POL,mass} = p_{IOM} < 0.0001$) were significant predictors of spray KE, while orientation ($p_{CAS\text{-}POL,mass} = 0.482$, $p_{IOM} = 0.184$) was not a significant predictor for either measurement method. The average overall efficiencies by mass for each spray/pressure combination calculated from the CAS-POL data and from the IOM filter weights are shown in Figure 3. For both measurement methods, the full cone spray had the highest KE (CAS-POL: 35.6%, IOM: 26.4%) and the air atomizing spray had the lowest KE (CAS-POL: 26.6%, IOM: 13.4%). On average, $KE_{CAS\text{-}POL,Mass}$ was 12% higher than the KE_{IOM}. Visual inspection of the data indicates that the CAS-POL measurements trend in a manner similar to the IOM measurements for each spray, which is supported by a reliability intraclass correlation coefficient (ICC) of 0.65 between the CAS-POL and IOM KE values. The IOM values had a coefficient of variation (CV) of 48.1% while the CAS-POL CV was 28.7%. These relatively large CV values were not unexpected; a previous study conducted in the same NIOSH test gallery found that static IOM samplers distributed across the gallery cross section could experience a CV of 24% due to position of the sampler alone.[49] Variation can also be attributed to the lack of uniformity of the dust within the test space. Higher air-speeds and coarser dust can contribute to high concentration gradients.[50–52]

The comparison of these two measurement techniques would not be complete without some discussion of expected operation and variability of each instrument. A previous laboratory investigation by NIOSH found that the IOM has an average CV of 4.6% for varying test conditions.[49] The current study was the first conducted by NIOSH using the CAS-POL and was not optimized for establishing an instrument CV, although this is expected to be done in future work. The CAS-POL was mounted so that the inlet extended into the free-stream air while the IOMs were mounted behind and above the top of the CAS-POL wing. This could have resulted in the IOMs experiencing irregular flow patterns contributing to the increased CV as compared to the CAS-POL. In this study, the IOM sampled isokinetically while the

CAS-POL sampled superisokinetically, meaning it was less likely to draw in large particles than the IOM[10]. For mass-based measurements, large particles have a larger effect on the measurement than small ones, therefore as the number of larger particles are reduced during the knockdown phase, the CAS-POL will be more susceptible to over-estimating the reduction in large particles than the IOM. The IOMs are prone to handling and weighing errors that don't apply to the CAS-POL collection process. However, both methods can be affected by the presence of water. The water in this study left a residue on the IOM filters that required a correction factor, while there was a potential for water particles to be misclassified as coal during the CAS-POL post-processing. In the case of the IOM, this could lead to an over- or under-estimation of the KE depending on the accuracy of the water blank measurement; for the CAS-POL, an underestimation of the KE could occur as outlined in the methods section. The CAS-POL is also prone to its interrogation windows becoming fouled over the course of testing. During the daily testing cycle the CAS-POL concentrations measured for each test phase decayed over the course of the day as the optics became dirty. This may be one reason that the CAS-POL KE_{mass} values were higher than the IOM—the additional loss to the fouling over time would make it look like more material was lost in a test than actually.

KECAS-POL: Particle count vs. calculated mass—Due to this study's use of particles with wide-ranging sizes, it is important to consider KE on a mass and count basis because a single large diameter particle will have greater influence on mass based calculations than many small particles. For example, it would take 8,000 1-μm coal particles to replicate the mass of a single 20-μm coal particle, meaning that knocking one large particle from the air will result in a large change in KE_{mass}. Conversely, when determining KE based on particle count, all particles carry the same weight in the calculation.

The overall $KE_{CAS\text{-}POL,mass}$ values for each spray, pressure, and orientation combination are shown in Figure 4. Overall, the full cone spray was found to have the highest efficiency (35.6%) followed by the wide flat fan (35.3%), and both were found to be significantly different in their performance compared to the air atomizing (26.6%), the narrow flat fan (27.9%) and the hydraulic atomizing (28.0%) sprays, which were the lowest performing sprays. The narrow hollow cone (33.9%) performance was significantly different to the air atomizing spray while wide hollow cone (33.3%) performance was not significantly different from any spray. From regression analysis, spray type ($p = 0.0001$, $\eta^2_{partial}=0.264$) and operating pressure ($p < 0.0001$, $\eta^2_{partial}=0.471$) were found to have a significant effect on KE, while orientation ($p = 0.48$, $\eta^2_{partial}=0.006$) was not significant. The main trends observed for pressure were an increase in pressure led to increased KE, and at elevated pressure the atomizing spray's KE was approximately 10% less than the single-fluid sprays.

The overall $KE_{CAS\text{-}POL,count}$ for each spray, pressure, and orientation combination are shown in Figure 5. Overall, the air atomizing spray was found to have the highest efficiency (17.2%), but its average performance was not significantly better than the other sprays—14.5% (wide flat fan), 13.5% (narrow hollow cone), 13.1% (full cone), 12.7% (narrow flat fan), 12.0% (wide hollow cone), and 11.8% (hydraulic atomizing). From regression analysis, operating pressure of the sprays was found to have a significant effect on the spray

performance ($p < 0.0001$, $\eta^2_{partial}=0.373$), while spray selection ($p = 0.0670$, $\eta^2_{partial}=0.123$) and orientation ($p = 0.0731$, $\eta^2_{partial}=0.036$) were not significant.

As evidenced above, an air atomizing spray would be a good choice if the goal was to remove as many particles as possible from the airstream, but a full cone would be selected if the desired outcome is the removal of the most dust mass from the airstream. Regardless of KE calculation method, pressure remains a significant predictor of spray performance with increased pressure resulting in increased KE and increased pressure correlates with a decrease in droplet diameter ($r_{SMD@0.3m} = -0.176$, $r_{SMD@0.6m} - 0.142$) and increase in droplet velocity ($r_{V@0.3} = 0.108$, $r_{V@0.3} = 0.216$).

KE by particle size

The $KE_{CAS\text{-}POL,count}$ and $KE_{CAS\text{-}POL,mass}$ values were calculated for each of the size bins described previously in the Methods section. Within each size bin, the $KE_{CAS\text{-}POL,count}$ and $KE_{CAS\text{-}POL,mass}$ were strongly correlated ($\rho \leq 4 = 0.829$, $\rho_{4\text{-}20} = 0.950$, $\rho_{>20} = 0.978$). $KE_{CAS\text{-}POL,mass}$ and $KE_{CAS\text{-}POL,count}$ for each spray and bin size are shown in Figure 6.

D ≤ μm—For both $KE_{CAS\text{-}POL,count}$ and $KE_{CAS\text{-}POL,mass}$ with particles with a diameter ≤4 μm, the air atomizing spray had the highest values, followed by the wide flat fan. For this size distribution, the least efficient spray using $KE_{CAS\text{-}POL,count}$ was the full cone, whereas the spray with the lowest $KE_{CAS\text{-}POL,mass}$ was the wide hollow cone spray. While the $KE_{CAS\text{-}POL,count}$ values for each spray were not significantly different for any spray, the air atomizing spray was significantly different from the wide hollow cone spray and the narrow flat fan when using $KE_{CAS\text{-}POL,mass}$. The $KE_{CAS\text{-}POL,count}$ and $KE_{CAS\text{-}POL,mass}$ for the narrow hollow cone and hydraulic atomizing sprays were not significantly different from any of the other sprays. Regression analysis found that operating pressure ($p < 0.0001$) was a significant predictor of $KE_{CAS\text{-}POL,count}$ and $KE_{CAS\text{-}POL,mass}$, with increasing pressure leading to increased KE. Spray type ($p = 0.0162$) was a significant predictor of $KE_{CAS\text{-}POL,mass}$ but was not significant ($p = 0.0577$) for $KE_{CAS\text{-}POL,count}$. The KE for particles ≤4 μm are most strongly correlated to the overall $KE_{CAS\text{-}POL,count}$ ($\rho_{count} = 0.915$, $\rho_{mass} = 0.865$).

4 < D ≤20 μm—For both $KE_{CAS\text{-}POL,count}$ and $KE_{CAS\text{-}POL,mass}$ in this size distribution, the full cone spray had the highest KE, followed by the wide flat fan spray. The least efficient sprays differed between the two KE calculation methods, with the narrow flat fan having the lowest $KE_{CAS\text{-}POL,mass}$, and the wide hollow cone having the lowest $KE_{CAS\text{-}POL,count}$. As with the smallest size bin, regression analysis found spray type ($p_{mass} = 0.0008$, $p_{count} = 0.0023$) and pressure ($p_{mass} = p_{count} < 0.0001$) to be significant factors, with positive correlation between pressure and KE. For particles between 4 and 20 μm, the KE values are strongly correlated to the overall $KE_{CAS\text{-}POL,mass}$ ($\rho_{count} = 0.918$, $\rho_{mass} = 0.937$).

D > 20 μm—There were no significant differences among the average performances of any of the sprays, and regression analysis found that only pressure ($p_{mass} = p_{count} < 0.0001$) had a significant effect on spray performance. The average knockdown efficiencies listed from highest to lowest for each were: wide flat fan, wide hollow cone, air atomizing, full cone,

narrow hollow cone, narrow flat fan, and the hydraulic atomizing. The KE for particles larger than 20 μm are also strongly correlated to the overall $KE_{CAS\text{-}POL,mass}$ (ρ_{count} = 0.805, ρ_{mass} = 0.798), but the correlations are not as strong as those observed for the 4–20 μm size bin.

KE by location

Timestamp values were used to sort the particles counted by the CAS-POL into groups based on location and then used to calculate $KE_{CAS\text{-}POL,mass}$ for each location sampled by the CAS-POL during the test. Four $KE_{CAS\text{-}POL,mass}$ maps were selected that show the overall trends observed in these maps (Figure 7). The full cone spray was the best performing spray and the air atomizing was the lowest performing spray using $KE_{CAS\text{-}POL,mass}$. However, both sprays show similar KE patterns, with the upper right (region 5) and lower left (region 11) corners having some of the lowest KE values across the investigation area. KE is maximized toward the left side of the tunnel at mid-height (regions 12–14). These trends held true for a majority of the sprays with some minor differences between cases, but the average standard deviation for each spray/pressure map was not significantly different between cases tested. The narrow flat fan spray had the largest difference in KE due to operating pressure changes. Again, the KE patterns change primarily in magnitude and not in relative location. One important difference observed in this particular spray is the presence of a sampling location that has a negative KE. The overall KE for the spray is positive, suggesting that dust-laden air is being moved into the lower left corner by the spray.

Conclusions

Several trends were observed in this study, as described below.

First, for all analyses, pressure was found to have a significant effect on spray performance for all particle sizes. Pressure increases are associated with an increase in water droplet velocity and a decrease in droplet diameter, both of which have been shown to contribute to increased capture efficiency.[19,22,53,54] Therefore, it is important to operate sprays at the highest pressure practical to achieve maximum performance. Spray orientation was not found to have a significant impact on spray knockdown performance.

Second, spray efficiencies increased as the dust particle size increased, which aligns with the findings of previous studies.[16,55,56] This is due to the different mechanisms that govern the capture efficiency of differently sized particles. Smaller particles (d < 1 μm) are primarily collected by diffusion, which has increasing efficiency with decreasing diameter, while large particles (d > 5 μm) are primarily collected through impaction, which increases in efficiency with increasing diameter.[8,57,58] In this study, the smallest bin size (d ≤ 4 μm) falls in the transition zone between small and large collection mechanics, possibly resulting in the low observed KE for this bin size. The two larger particle size bins used in this study followed the trend of increased efficiency with increasing particle size.

Finally, this study demonstrated that, while the measurements of KE by CAS-POL and IOM samplers are not interchangeable in their current form, the CAS-POL is able to capture the

impact of spray selection, operating pressure, and spray orientation on KE in a manner similar to IOM samplers. The overall KE values between the CAS-POL and the IOM samplers trend well for 13 out of 14 conditions, with the narrow hollow cone operating under high pressure having the most marked difference between the two measurement techniques. This may be due to a problem with the water blank taken for this condition, as the filter mass for this condition did not follow the trends observed in the other water blanks. Additionally, the IOM samplers are subject to error from the handling and processing of the filters, which may contribute to the increased CV as compared to the CAS-POL. The CAS-POL reduces the period between test completion and data analysis because it does not require the same equilibration process required for the IOM samplers, reducing the time from test completion to data visualization to hours rather than days.

One limitation of the CAS-POL is that its KE measurement is not interchangeable with the IOM KE. However, this limitation does not outweigh the added detail the CAS-POL is able to provide. First, the average difference between the CAS-POL KE and IOM KE was only 12%. Previous work has shown that 30% KE for a control in the laboratory is the threshold at which the control may begin to produce a measurable result in the field.[59,60] The primary goal of most industrial hygiene research is to maximize a control's efficiency and, combined with the above guidelines, a difference of 12 percentage points between measurement techniques is not large enough to significantly affect design decisions. Second, the lean flammability limit concentration for low volatile bituminous coal remains relatively constant for particles less than 10 μm and then increases rapidly for particles over 20 μm.[61] Therefore, it is important to ensure that the particles that pose the greatest risk are being measured when establishing a FCD control KE. Under the conditions tested, the CAS-POL is sampling approximately 93% of the particles under 10 μm and 77% of the particles under 20 μm based on isokinetic sampling theory.[62]

As mentioned above, the CAS-POL can provide additional information about the control KE as compared to the IOM. The IOMs in this study were fitted with nozzles allowing them to operate isokinetically, but they are still only able to provide a test averaged mass measurement. In comparison, the CAS-POL is able to provide post-test customizable size segregated KE values for the different test conditions. A more detailed understanding for a spray KE over the entire size range of FCD allows researchers to achieve more fine-tuned controls for deployment in the field. Since the CAS-POL position is tracked and the data for each particle is timestamped, the KEs for different areas over the entire test cross section can be examined. As the investigation area in this test was rather small (1.5 m^2) compared to the full gallery (16 m^2) and was relatively rectangular and free of flow disturbances, the KE across the tunnel did not vary greatly. Future tests will apply the results of this study utilizing multiple sprays in the full longwall gallery cross section in order to develop a control capable of reducing the amount of FCD that reaches the return. In this setting, large variations in flow are expected, and proper placement of sprays to maximize KE and minimize gaps in the control is important.

In summary, this study found that operating pressure was the most important consideration when attempting to maximize KE and that orientation into or against the airflow did not have a large effect on KE. In general, the single-fluid mining sprays, with the exception of

the hydraulic atomizing, achieved a similar performance that was above that of the air atomizing spray in the presence of FCD. A new instrument (CAS-POL) was used in conjunction with gravimetric samplers (IOM) in each test, and although the KEs measured by each were significantly different in magnitude, the responses in KE to changing test conditions were similar enough to warrant further use of the CAS-POL in future studies. The CAS-POL was also able to provide insight into the KE for different particle size distributions and locations within the test space, which will aid researchers in future studies aimed at developing a full-scale water curtain that will reduce the amount of airborne FCD able to settle in the mine airways, thus reducing the risk of coal dust explosions in underground coal mines.

Acknowledgments

The authors would like to thank the following people for their contributions to this work: Teresa Barone, Jay Colinet, Jason Driscoll, Jon Hummer, Andrew Mazzella, Larry Patts, Jim Rider, Elaine Rubenstein, Milan Yekich, and Jeanne Zimmer.

References

1. Abbasi T, Abbasi SA. Dust explosions–Cases, causes, consequences, and control. J Haz Mater. 2007; 140:7–44.
2. Nagy, J. The Explosion Hazard in Mining. Pittsburgh, PA: U.S. Department of Labor Mine Safety amd Health Administration; 1981. IR 1119
3. Centers for Disease Control and Prevention. Coal Mining Disasters: 1839 to Present. Available at https://www.cdc.gov/niosh/mining/statistics/content/coaldisasters.html (accessed September 30, 2016)
4. Mine Safety and Health Administration. Coal Fatalities for 1900 through 2016. Available at http://arlweb.msha.gov/stats/centurystats/coalstats.asp (accessed January 30, 2017)
5. Maintenance of Incombustible Content of Rock Dust. Code of Federal Regulation Title. 2011; 30:561–562. Part 75.403.
6. Baron PA. Factors affecting aerosol sampling. NIOSH Manual on Analytical Methods (5th). 2016
7. Fredericks S, Saylor JR. Parametric investigation of two aerosol scavenging models in the inertial regime. J Aerosol Sci. 2016; 101:34–42.
8. Kim HT, Jung CH, Oh SN, Lee KW. Considering diffusion, interception, and impaction. Environ Eng Sci. 2001; 18(2):125–136.
9. Beard KV. Experimental and numerical collision efficiencies for submicron particles scavenged by small raindrops. J Atmos Sci. 1974; 31:1595–1603.
10. Hinds, WC. Aerosol Technology: Properties, Behavior, and Measurement of Airborne Particles. 2nd. New York: John Wiley & Sons; 1999.
11. Courtney W, Cheng L. Control of respirable dust by improved water sprays. Respir Dust Control Technol Transf Semin. 1977; 92–108
12. McPherson, MJ. Subsurface Ventilation and Environmental Engineering. Chapman & Hall; 1993.
13. Tobergte DR, Curtis S. Type of wet scrubber. J Chem Inf Model. 2013; 53(9):1689–1699. [PubMed: 23800267]
14. Tomb TF, Emmerling JE, Kellner RH, Tomb TF, Emmerling JE, Kellner RH. Collection of airborne coal dust by water spray in a horizontal duct collection of airborne coal dust by water spray in a horizontal duct. Am Ind Hyg Assoc J. 1972; 33(11):715–721. [PubMed: 4661862]
15. Cheng L. Collection of airborne dust by water sprays. Ind Eng Chem Process Des. 1973; 12(3): 221–225.
16. Walton WH, Woolcock A. The suppression of airborne dust by water spray. Int J Air Pollut. 1960; 3(1):129–153. [PubMed: 13783012]

17. Ruggieri, SK.Muldoon, TL.Schroeder, W.Babbitt, C., Rajan, S., editors. U.S Bureau of Mines. Optimizing water sprays for dust control on longwall shearer faces. Foster-Miller, Inc.; 1983. Contract No. J0308019
18. Jayaraman N, Schroeder W, Kissel F. Studies of dust knockdown by water sprays using a full-scale model mine entry. Trans Soc Min Eng. 1986; 278:1875–1882.
19. Chander, S., Alaboyun, AR., Aplan, FF., Section, MP. On the mechanism of capture of coal dust particles by sprays. In: Frantz, R., Ramani, R., editors. Proc of the 3rd Symposium on Respirable Dust in the Mineral Industries. Littleton, CO: Society for Mining, Metallurgy, and Exploration, Inc; 1991. p. 193-202.
20. McCoy JF, Schroeder WE, Rajan SR, Ruggieri SK, Kissel FN. New laboratory measurement method for water spray dust control effectiveness. Am Ind Hyg Assoc J. 1985; 46(12):735–740.
21. U.S. Department of the Interior. Dust Knockdown Performance of Water. U.S. Bureau of Mines; Jul. 1982 Technology News No. 150
22. Pollock D, Organiscak J. Airborne dust capture and induced airflow of various spray nozzle designs. Aerosol Sci Technol. 2007; 41(7):711–720.
23. Hertzberg, M., Cashdollar, KL. Industrial Dust Explosions. ASTM International; 1987. Introduction to dust explosions.
24. Man CK, Harris ML. Participation of large particles in coal dust explosions. J Loss Prev Process Ind. 2014; 27(1):49–54.
25. Cashdollar KL. Coal dust explosibility. J Loss Prev Process Ind. 1996; 9(1):65–76.
26. Reid JS, Jonsson HH, Maring HB, et al. Comparison of size and morphological measurements of coarse mode dust particles from Africa. J Geophys Res-Atmos. 2003; 108(D19):9-1–9-28.
27. Whitby KT, Vomela RA. Response of single particle optical counters to nonideal particles. Environ Sci Technol. 1967; 1(10):801–814. [PubMed: 22148376]
28. Liu BYH V, Marple A, Whitby KT, Barsic NJ. Size distribution measurement of airborne coal dust by optical particle counters. Am Ind Hyg Assoc J. 1974; 35(8):443–451. [PubMed: 4417069]
29. Baumgardner D, Jonsson H, Dawson W, O'Connor D, Newton R. The cloud, aerosol and precipitation spectrometer: A new instrument for cloud investigations. Atmos Res. 2001; 59–60:251–264.
30. Baumgardner D, Newton R, Krämer M, et al. The cloud particle spectrometer with polarization detection (CPSPD): A next generation open-path cloud probe for distinguishing liquid cloud droplets from ice crystals. Atmos Res. 2014; 142:2–14.
31. Kobayashi H, Hayashi M, Shiraishi K, et al. Development of a polarization optical particle counter capable of aerosol type classification. Atmos Environ. 2014; 97:486–492.
32. Glen A, Brooks SD. A new method for measuring optical scattering properties of atmospherically relevant dusts using the Cloud and Aerosol Spectrometer with Polarization (CASPOL). Atmos Chem Phys. 2013; 13(3):1345–1356.
33. Jurányi Z, Burtscher H, Loepfe M, Nenkov M, Weingartner E. Dual-wavelength light-scattering technique for selective detection of volcanic ash particles in the presence of water droplets. Atmos Meas Tech. 2015; 8:5213–5222.
34. Barone, TL., Seaman, ECE., Baran, AT., et al. Real-time sizing of airborne coarse coal dust. In: Brune, J., editor. 16th Annual Mine Ventilation Symposium Proceedings. 2017. 16th Annu Mine Vent Symp Proc
35. Shahan, MR., Seaman, CE., Beck, TW., Colinet, JF., Mischler, SE. SME Annual Meeting. Denver, CO: Society of Mining Engineering; 2017. Characterization of airborne float coal dust emitted during continuous mining, longwall mining, and belt transport.
36. Janisko SJ, Colinet JF, Patts JR, Barone T, Patts LD. Field evaluation of an inline wet scrubber for reducing float coal dust on a continous miner section. Min Eng. 2016; 68(12):63–68. [PubMed: 28018004]
37. Method 1: Sample and Velocity Traverses for Stationary Sources. Code of Federal Regulation Title. 1994; 40 Part 60 Appendix A.
38. Curtis DB, Meland B, Aycibin M, et al. A laboratory investigation of light scattering from representative components of mineral dust aerosol at a wavelength of 550 nm. J Geophys Res. 2008; 113:1–15.

39. Johnson B, Turnbull K, Brown P, et al. In-situ observations of volcanic ash clouds from the FAAM aircraft during the eruption of Eyjafjallajökull in 2010. J Geophys Res Atmos. 2012; 117(D20): 2156–2202.
40. Sassen K, Liou KN. Scattering of polarized laser light by water droplet, mixed-phase and ice crystal clouds. Part I: Angular scattering patterns. J Atmos Sci. 1979; 36(5):838–851.
41. Spinrad RW, Brown J. Effects of asphericity on single-particle polarized light scattering. Appl Opt. 1993; 32(30):6151–6158. [PubMed: 20856444]
42. Muñoz O, Hovenier JW. Laboratory measurements of single light scattering by ensembles of randomly oriented small irregular particles in air. A review. J Quant Spectrosc Radiat Transf. 2011; 112(11):1646–1657.
43. Bohren, CF., Huffman, DR. Absorption and Scattering of Light by Small Particles. New York: John Wiley & Sons; 1983. Absorption and scattering by a sphere.
44. Havemann S, Baran AJ. Extension of T-matrix to scattering of electromagnetic plane waves by non-axisymmetric dielectric particles – Application to hexagonal ice cylinders. J Quant Spectrosc Radiat Transf. 2001; 70:139–158.
45. Hesse E, McCall DS, Ulanowski Z, Stopford C, Kaye PH. Application of RTDF to particles with curved surfaces. J Quant Spectrosc Radiat Transf. 2009; 110(14–16):1599–1603.
46. Huang H, Wang K, Bodily DM, Hucka VJ. Density measurements of argonne premium coal samples. Energy Fuels. 1995; 9(1):20–24.
47. Bartley DL, Chen C, Song R, et al. Respirable aerosol sampler performance testing. Am Ind Hyg Assoc J. 1994; 55(11):1036–1046.
48. Soderholm SC. Proposed international cconventions for particle size-selective sampling. Ann Occup Hyg. 1989; 33(3):301–320. [PubMed: 2802448]
49. Patts JR, Barone TL. Comparison of coarse coal dust sampling techniques in a laboratory-simulated long-wall section. J Occup Environ Hyg. 2016
50. Witscheger O, Wrobel R, Fabriès JF, Görner P, Renoux A. A new experimental wind tunnel facility for aerosol sampling investigations. J Aerosol Sci. 1997; 28(5):833–851.
51. Kenny LC, Aitken R, Chalmers C, et al. A collaborative European study of personal inhalable aerosol sampler performance. Ann Occup Hyg. 1997; 41(2):135–153. [PubMed: 9155236]
52. Cheng YS, Irshad H, McFarland A, Su WC, Zhou Y, Barringer D. An aerosol wind tunnel for evaluation of massive-flow air samplers and calibration of Snow White sampler. Aerosol Sci Technol. 2004; 38(11):1099–1107.
53. Kost, JA.Saltsman, RD., duBreuil, R., editors. U.S. Bureau of Mines. Water Spray Systems for Control of Respirable Dust on a Longwall Plow Underground Investigation and Dust Tunnel Evaluation. Bituminous Coal Research, Inc.; Jan. 1979 Contract No. HO242013
54. Beck TW, Seaman CE, Shahan MR, Mischler SE. Open-air sprays for capturing and controlling airborne float coal dust on longwall faces. Min Eng. 2018; 70(1):42–48. [PubMed: 29348700]
55. Starr JR, Mason BJ. The capture of airborne dust by water spray. Q J R Meterol Soc. 1966; 92(394):490–499.
56. Charinpanitkul T, Tanthapanichakoon W. Deterministic model of open-space dust removal system using water spray nozzle: Effects of polydispersity of water droplet and dust particle. Sep Purif Technol. 2011; 77(3):382–388.
57. Perry, RH., Green, DW. Perry's Chemical Engineers' Handbook. 6th. New York: McGraw-Hill Publishing Company Inc; 1984.
58. The McIlvaine Scrubber Manual. Northbrook, IL: The McIlvaine Company; 1995.
59. Kost, JA., editor. U.S. Bureau of Mines. Refinement and Evaluation of Basic Longwall Dust-control Techniques. Bituminous Coal Research, Inc.; Sep. 1984 Contract No. AI01-81FE0016
60. UK National Coal Board. Methods of Reducing Dust Formation and Improving Dust Suppression on Longwall Faces. Mining Research and Development Establishment; 1981. ESCS Project 7256-12/003/08
61. Hertzberg M, Cashdollar KL, Ng DL, Conti RS. Domains of flammability and thermal ignitability for pulverized coals and other dusts: Particle size dependences and microscopic residue analyses. 19th Symp Combust. 1982; 19(1):1169–1180.

62. Belyaev SP, Levin LM. Techniques for collection of representative aerosol samples. J Aerosol Sci. 1974; 5(4):325–338.

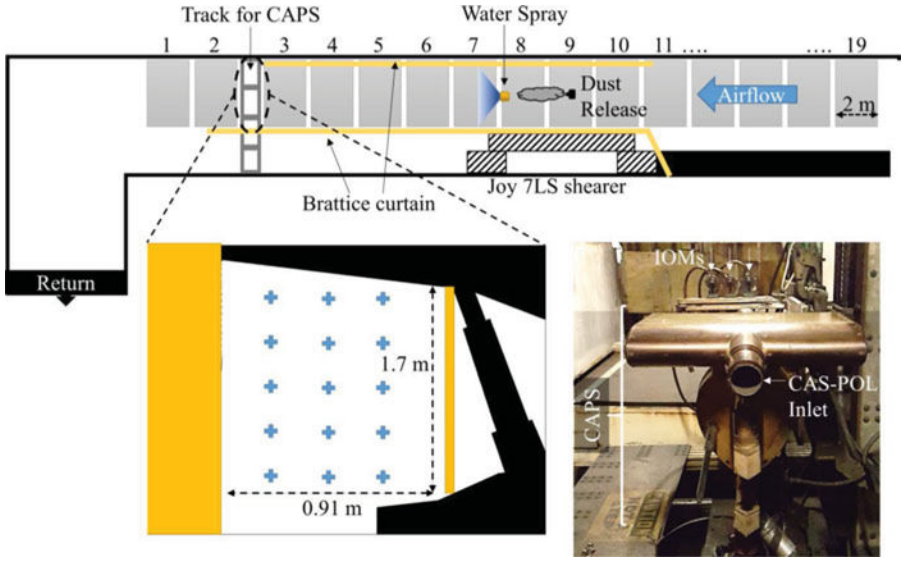

Figure 1.

Schematic of the NIOSH longwall gallery with cross section of the gallery after brattice curtain created a rectangular tunnel and picture of the CAPS and IOM instruments. The plus marks indicate the stationary measurement locations during each test.

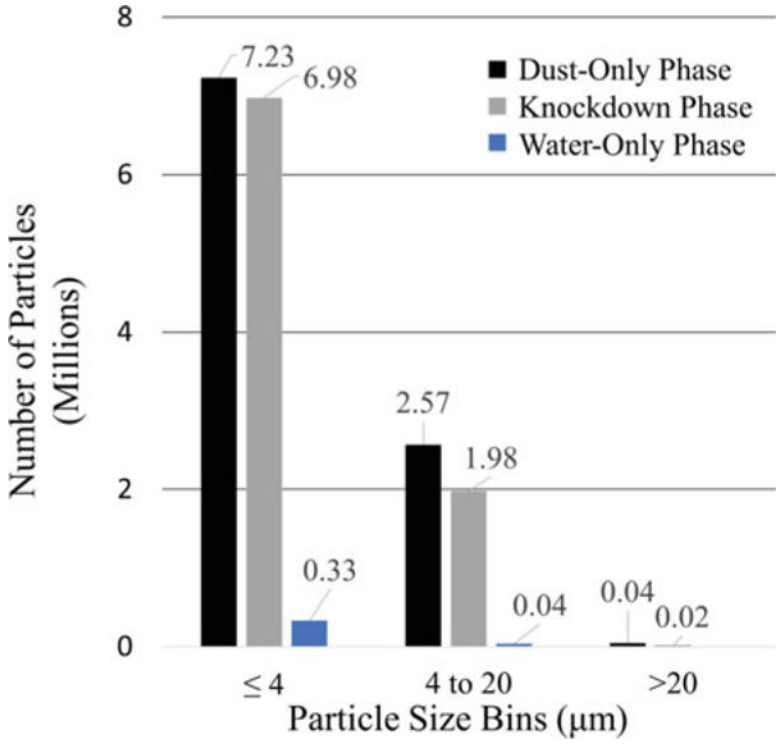

Figure 2.
Number of particles used to calculate efficiencies for each dust particle size bin.

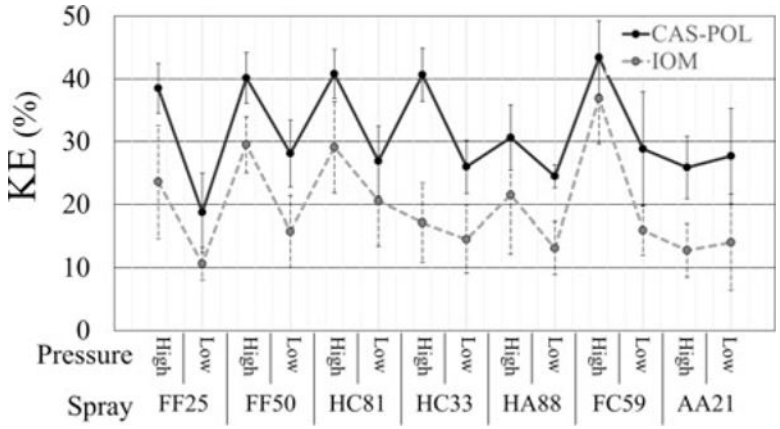

Figure 3.

Graph of overall average KE calculated from estimated mass measured by the CAS-POL and from actual mass of IOM filters for each spray and pressure combination (standard deviation represented by the error bars).

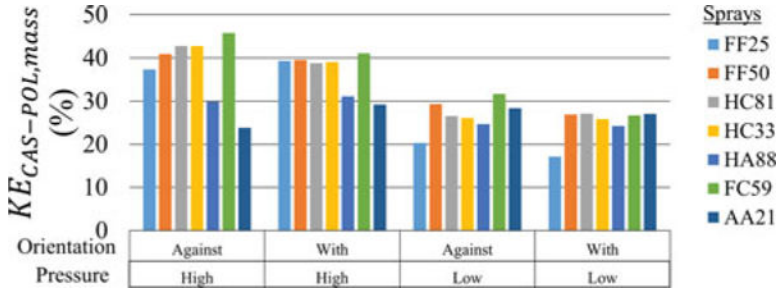

Figure 4.

Graph of overall efficiencies based on mass of particles calculated from CAS-POL data for each spray, pressure, and orientation combination.

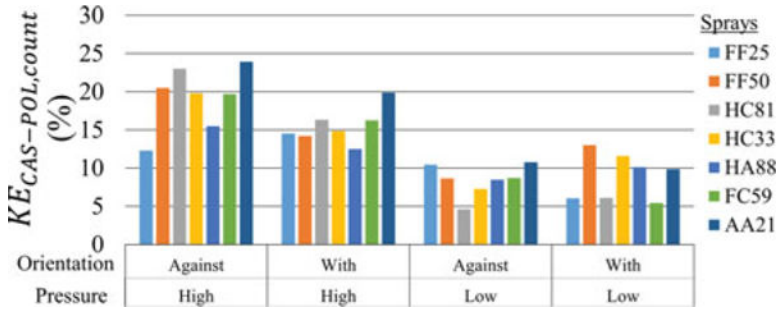

Figure 5.

Graph of overall efficiencies based on particle count from the CAS-POL for each spray, pressure, and orientation combination.

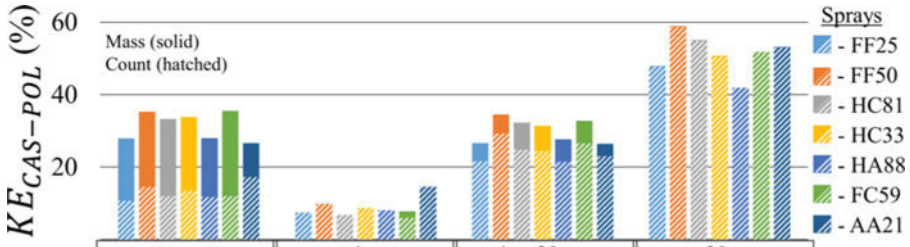

	KE_{Mass}	KE_{Count}	KE_{Mass}	KE_{Count}	KE_{Mass}	KE_{Count}	KE_{Mass}	KE_{Count}
FF25	27.9	10.7	6.2	7.5	26.6	21.6	47.9	47.8
FF50	35.3	14.5	9.9	9.8	34.6	29.2	58.9	58.6
HC81	33.3	12.0	5.3	6.8	32.3	24.8	55.0	54.8
HC33	33.9	13.5	6.5	8.8	31.4	24.4	50.7	50.5
HA88	28.0	11.8	7.3	8.1	27.7	21.4	40.1	42.0
FC59	35.6	12.0	7.8	6.0	32.8	26.6	51.4	51.8
AA21	26.6	17.2	13.5	14.6	26.4	23.0	53.2	53.0

Figure 6.

Graph and data table of KE for each size distribution of coal dust as calculated by mass (solid bars) and particle count (hatched bars) from CAS-POL size data.

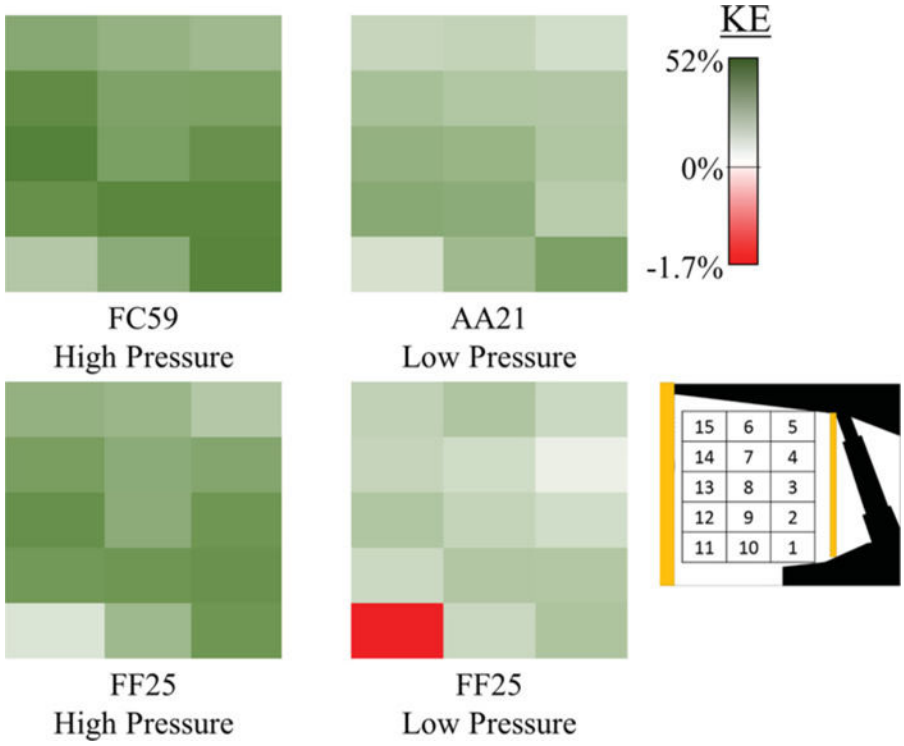

Figure 7.

$KE_{CAS\text{-}POL,mass}$ maps generated using CAS-POL mass data for the most efficient spray, full cone (FC59), the least efficient spray, air atomizing (AA21), and the spray that had the largest change due to pressure effects, narrow flat fan (FF25).

Table 1

Table of spraying system sprays tested.

Spray Designation	Spray Name	Spray Type	Performance Specifications				
			Angle	Pressure (kPa)	Water/(Air) Flow Rate (lpm)	SMD at 0.3 (0.6) m (μm)	Velocity at 0.3 (0.6) m (m/s)
FF25	FlatJet Nozzle no. TT2506	Flat Fan	25°	552 1104	3.22 4.16	244.3 (252.3) 198.4 (201.2)	13.3 (9.8) 21.2 (14.4)
FF50	FlatJet Nozzle No. TT5006	Flat Fan	50°	552 1104	3.26 4.16	234.6 (220.8) 195.3 (196.9)	14.7 (8.8) 23.5 (14.5)
HC81	WhirlJet Nozzle No. TTD6-45	Hollow Cone	81°	552 1104	3.14 4.54	73.8 (89.1) 60.1 (82.6)	2.6 (1.3) 3.3 (2.2)
HC33	WhirlJet Nozzle No. TTD4-46	Hollow Cone	33°	552 1104	2.95 3.63	138.3 (109.5) 98.2 (91.6)	8.3 (4.9) 11.7 (8.0)
HA88	Hydraulic Atomizing Nozzle No. LNN14	Full Cone	88°	552 1104	— —	— —	— —
FC59	SpiralJet Nozzle No. GG3	Full Cone	59°	552 1104	2.84 3.63	129.3 (125.8) 106.1 (108.5)	6.3 (4.3) 9.7 (7.8)
AA21	Air Atomizing Nozzle No. J-SU22	Twin-Fluid Full Cone	21°	172 air/water 345 air/water	1.92 (99.1) 2.60 (163)	166.0 (165.0) 143.0 (146.0)	13.8 (8.5) 22.4 (12.5)

J Occup Environ Hyg. Author manuscript; available in PMC 2019 March 01.